Cerebral Cortex December 2008;18:2735–2747
doi:10.1093/cercor/bhn041
Advance Access publication April 9, 2008

Functional Connectivity of Human Striatum: A Resting State fMRI Study

A. Di Martino[1,2], A. Scheres[3], D.S. Margulies[1], A.M.C. Kelly[1], L.Q. Uddin[1], Z. Shehzad[1], B. Biswal[4], J.R. Walters[5], F.X. Castellanos[1,6] and M.P. Milham[1]

[1]Phyllis Green and Randolph Cowen Institute for Pediatric Neuroscience at the NYU Child Study Center, New York, NY 10016, USA, [2]Division of Child and Adolescent Neuropsychiatry, Department of Neuroscience, University of Cagliari, 09126 Cagliari, Italy, [3]Department of Psychology, University of Arizona, Tucson, AZ 85701, USA, [4]Department of Radiology, University of Medicine and Dentistry of New Jersey, Newark, NJ 07103, USA, [5]The Neurophysiological Pharmacology Section, National Institute of Neurological Disorders and Stroke, Bethesda, MD 20892, USA and [6]Nathan Kline Institute for Psychiatric Research, Orangeburg, NY 10962, USA

A. Di Martino and A. Scheres contributed equally to the manuscript.

Classically regarded as motor structures, the basal ganglia subserve a wide range of functions, including motor, cognitive, motivational, and emotional processes. Consistent with this broad-reaching involvement in brain function, basal ganglia dysfunction has been implicated in numerous neurological and psychiatric disorders. Despite recent advances in human neuroimaging, models of basal ganglia circuitry continue to rely primarily upon inference from animal studies. Here, we provide a comprehensive functional connectivity analysis of basal ganglia circuitry in humans through a functional magnetic resonance imaging examination during rest. Voxelwise regression analyses substantiated the hypothesized motor, cognitive, and affective divisions among striatal subregions, and provided in vivo evidence of a functional organization consistent with parallel and integrative loop models described in animals. Our findings also revealed subtler distinctions within striatal subregions not previously appreciated by task-based imaging approaches. For instance, the inferior ventral striatum is functionally connected with medial portions of orbitofrontal cortex, whereas a more superior ventral striatal seed is associated with medial and lateral portions. The ability to map multiple distinct striatal circuits in a single study in humans, as opposed to relying on meta-analyses of multiple studies, is a principal strength of resting state functional magnetic resonance imaging. This approach holds promise for studying basal ganglia dysfunction in clinical disorders.

Keywords: basal ganglia, caudate, fMRI, functional connectivity, nucleus accumbens, putamen, resting state

Introduction

Classically regarded as motor structures (Kemp and Powell 1971), the basal ganglia have been implicated in a variety of motor-related functions such as motor selection, preparation, and execution (e.g., Gerardin et al. 2004). Consistent with this role, human lesion studies and clinical studies of neurological populations such as Parkinson's disease, Tourette's syndrome, and Huntington's disease have implicated basal ganglia dysfunction in motor abnormalities such as rigidity, tremor, akinesia, choreiform movements, and tics (Bhatia and Marsden 1994; Albin and Mink 2006; Montoya et al. 2006; Wichmann and DeLong 2006).

Nonhuman primate (Selemon and Goldman-Rakic 1985; Alexander et al. 1986; Cavada and Goldman-Rakic 1991; Middleton and Strick 2000b; Haber 2003) and neuroimaging studies have suggested a broader conceptualization of the role of the basal ganglia, implicating these structures in a diverse array of executive/cognitive control (e.g., verbal and spatial working memory, response inhibition, task switching, reasoning, and planning; Postle and D'Esposito 2003; Crottaz-Herbette et al. 2004; Garavan et al. 2006; Monchi et al. 2006; Rubia et al. 2006), and reward-related/motivational processes (e.g., prediction error; feedback-related reinforcement; reward anticipation; incentive salience; McClure et al. 2003; Ernst et al. 2005; Knutson and Cooper 2005; Delgado 2007). Basal ganglia dysfunction has also been implicated in psychopathological conditions associated with deficits in executive and motivational processes, including major depressive disorder, bipolar disorder, schizophrenia, substance use disorders, obsessive compulsive disorder, and attention-deficit/hyperactivity disorder (ADHD) (Castellanos et al. 1996; Lafer et al. 1997; Stein et al. 2000; Shenton et al. 2001; Sagvolden et al. 2005; Sonuga-Barke 2005; Chang et al. 2007; Wessa et al. 2007).

In recent years researchers have begun to appreciate distinctions within the classical basal ganglia structures (e.g., caudate, putamen, globus pallidus), as well as the functionally distinct neural circuits associated with different basal ganglia subregions. For example, specific reward related processes have been differentially attributed to ventral versus dorsal striatum with the former implicated in prediction of future rewards, and the latter in maintaining information about reward outcomes (O'Doherty et al. 2004). Similarly, different aspects of movement are represented in distinct putamen and caudate regions (Gerardin et al. 2004).

Given that most of our knowledge of basal ganglia circuitry is based on animal circuit tracing studies (Selemon and Goldman-Rakic 1985; Cavada and Goldman-Rakic 1991; Middleton and Strick 1994; Ferry et al. 2000; Haber et al. 2000, 2006; Middleton and Strick 2002), investigators have recently attempted to examine basal ganglia subdivisions and circuitry in humans, with some success, though with notable limitations. For instance, 2 preliminary diffusion tensor imaging (DTI) studies (Lehericy et al. 2004; Leh et al. 2007) confirmed the segregation of corticostriatal connections, particularly with frontal cortex. However, in contrast with nonhuman primate data (Kunishio and Haber 1994; Haber et al. 2006), ventral

striatum was not found to be connected with cingulate cortex. This negative result was not unexpected, as DTI fiber tract reconstruction is less accurate for complex fiber directions such as those in frontal lobe, and the samples in both studies were very small. Finally, as anatomical studies, the DTI investigations by Lehericy et al. and Leh et al. do not provide direct information about functional networks.

An alternative approach to describing striatal functional networks involved a meta-analysis of 126 functional magnetic resonance imaging (fMRI) and positron-emission tomography human neuroimaging studies (Postuma and Dagher 2006). The meta-analysis demonstrated functionally distinct anatomical areas within striatum. However, orbitofrontal cortex (OFC) was not found to be coactivated with ventral striatum, despite specific predictions regarding its role in emotion/motivation, and its documented anatomical connectivity with ventral striatum shown in animal studies (Ferry et al. 2000; Haber et al. 2006).

Our goal in this study was to map basal ganglia circuitry in humans using recently developed resting state functional connectivity techniques (Fox and Raichle 2007; Margulies et al. 2007), which rely on detecting coherent patterns of spontaneous activity. This approach appears to delineate entire functional networks which are typically observed in task activation-based studies in a more fragmentary manner (Fox and Raichle 2007). Additionally, resting state scanning avoids potential confounds or limitations encountered in task-based approaches (e.g., practice, ceiling or floor effects, or differential performance levels) (Greicius et al. 2003; Beckmann et al. 2005; Fransson 2005; DeLuca et al. 2006; Damoiseaux et al. 2006; Dosenbach et al. 2007; Fair et al. 2007). Taking the anterior cingulate cortex (ACC) as an initial example, we recently demonstrated that resting state analyses can provide a comprehensive examination of functional connectivity in a structurally and functionally heterogeneous structure (Margulies et al. 2007). Our analyses revealed more fine-grained patterns of differentiation among ACC subregions than appreciated in task-based studies (Paus et al. 1998; Bush et al. 2000; Kiehl et al. 2000; Braver et al. 2001; van Veen et al. 2001; Weissman et al. 2004; Milham and Banich 2005).

In the present work, we subdivide striatal subregions in Talairach space following Postuma and Dagher (2006) by defining 6 seed regions: dorsal caudate (DC), ventral caudate (superior), ventral caudate/nucleus accumbens (inferior), dorsal rostral putamen (DRP), dorsal caudal putamen (DCP), and ventral rostral putamen (VRP) (see Fig. 1 and Table 1).

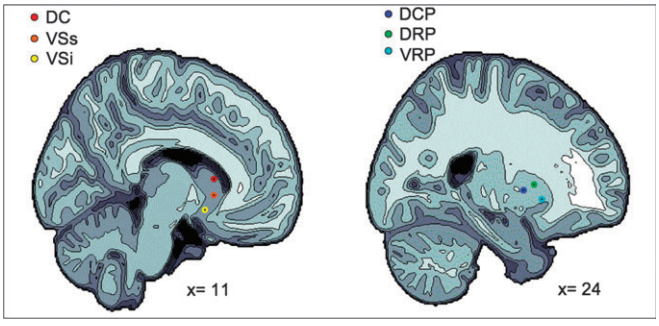

Figure 1. Representation of the 6 striatal regions of interest. The left and the right panels show the projection of the 3 caudate regions (i.e., DC; VSs; VSi), and the 3 putamen regions (i.e., DCP; DRP; VRP), respectively, onto sagittal brain views for $x = 11$ and $x = 24$.

Consistent with prior work we hypothesized that differential patterns of connectivity would be noted across the 6 striatal subregions examined. More specifically, for the putamen, we predicted that the rostral division would show greater connectivity with regions involved in cognition than the caudal division, reflecting the commonly cited cognitive/motor distinction (Parent and Hazrati 1995). Among the caudate subregions, we hypothesized that 1) the inferior ventral striatal region would exhibit greater connectivity with limbic and orbitofrontal regions (not previously detected in the Postuma and Dagher meta-analysis) than with dorsal regions involved in cognition, 2) that dorsal caudate would show greater connectivity with dorsolateral prefrontal and parietal cortices than with ventral regions involved in affective processing, and 3) that superior ventral striatum (VSs) would correlate with intermediate regions along the ventral-dorsal axis. As in the example of the ACC, for each of these distinctions, we expected to find more detailed patterns of functional connectivity than have previously been appreciated in task-based fMRI human studies.

Methods

Participants

Thirty-five right-handed native English-speaking participants were included (20 males; mean age: 28.4 ± 8.5 years). Subjects had no history of psychiatric or neurological illness as confirmed by a psychiatric clinical assessment. The study was approved by the institutional review boards of the New York University School of Medicine and New York University. Signed informed consent was obtained prior to participation.

Data Acquisition

A Siemens Allegra 3.0 Tesla scanner equipped for echo planar imaging (EPI) was used for data acquisition. For each participant, we collected 197 contiguous EPI functional volumes (time repetition [TR] = 2000 ms; time echo [TE] = 25 ms; flip angle = 90, 39 slices, matrix = 64 × 64; field of view [FOV] = 192 mm; acquisition voxel size = 3 × 3 × 3 mm). Complete cerebellar coverage was not obtained for all participants. Thus, only those cerebellar regions covered by the EPI array in all subjects were included in the statistical analyses described below (see Supplementary Fig. 1 for depiction of cerebellar coverage). During the scan, participants were instructed to rest with their eyes open while the word "Relax" was centrally projected in white, against a black background. For spatial normalization and localization, a high-resolution T_1-weighted anatomical image was then acquired using a magnetization prepared gradient echo sequence (TR = 2500 ms; TE = 4.35 ms; time of inversion = 900 ms; flip angle = 8; 176 slices, FOV = 256 mm).

Image Preprocessing

Data processing was carried out using both analysis of functional neuroimaging (AFNI) (http://afni.nimh.nih.gov/afni/) and fMRIb

Table 1
Coordinates for striatal regions of interest

	x	*y*	*z*
VSi	(±) 9	9	−8
VSs	(±) 10	15	0
DC	(±) 13	15	9
DCP	(±) 28	1	3
DRP	(±) 25	8	6
VRP	(±) 20	12	−3

Note: Coordinates for right and left hemisphere seeds defined in the MNI stereotaxic space.

software library (FSL) (www.fmrib.ox.ac.uk). Image preprocessing using AFNI consisted of 1) slice time correction for interleaved acquisitions, using Fourier interpolation, 2) 3D motion correction (3D volume registration using least-squares alignment of 3 translational and 3 rotational parameters), and 3) despiking (squashing of extreme time series outliers using a hyperbolic tangent function). Preprocessing using FSL consisted of 4) spatial smoothing (Gaussian kernel of full width half maximum 6 mm), 5) temporal highpass filtering (Gaussian-weighted least-squares straight line fitting with sigma = 100.0 s), and 6) temporal lowpass filtering (Gaussian filter with half width at half maximum = 2.8 s).

Functional Connectivity: Region of Interest Selection and Seed Generation

The goal of the present study was to provide a comprehensive survey of functional connectivity of striatal architecture. We 1st distinguished ventral striatum and dorsal caudate (using $z < 7$ mm as marker for ventral striatum and $z > 7$ mm as marker for dorsal caudate, following Postuma and Dagher (2006). Second, we divided the ventral striatum into inferior and superior regions (VSi and VSs, respectively) corresponding to nucleus accumbens and ventral caudate, respectively (Heimer and Alheid 1991; Drevets et al. 1999). Third, to confirm the putamen's dorsal–ventral coactivation gradient previously described by Postuma and Dagher (2006), putamen was divided into dorsal and ventral regions (using $z = 2$ mm as the boundary per Postuma and Dagher 2006). Finally, in order to obtain a finer parcellation, we identified dorsal caudal, dorsal rostral, and ventral rostral putamen subregions. The globus pallidus, substantia nigra, and subthalamic nucleus were excluded in the present examination due to limitations of the spatial resolution of the data acquired (3 × 3 × 3 mm), which was selected to maximize brain coverage. The seed coordinates were 1st selected based on the atlas space of Talairach and Tournoux (1988). Second, they were transformed into the Montreal Neurological Institute (MNI) space using the algorithm implemented by Brett (1999). Third, each set of transformed coordinates was visually inspected, and, when necessary, manually corrected to be centered within gray matter (using the 152 brain standard MNI gray matter provided by FSL) with a minimum Euclidean distance requirement between any 2 regions of 8 mm (see Table 1 for seed coordinates; see Fig. 1 and Supplementary Fig. 2 for seed locations). One set of seeds was created for each hemisphere (each seed covered 123 voxels in 1 × 1 × 1 mm space with a radius of 3.5 mm). In order to obtain the time series for each seed, for each subject, we 1) transformed each subject's time series into MNI space using a 12 degree of freedom linear affine transformation implemented in FLIRT (voxel size = 1 × 1 × 1 mm), and 2) calculated the mean time series for each seed by averaging across all voxels within the seed.

Functional Connectivity: Nuisance Signals

The time series of 9 nuisance signals were identified for inclusion in our analyses: global signal, white matter (WM), cerebrospinal fluid (CSF), and 6 motion parameters. As the global signal is thought to reflect a combination of physiological processes (such as cardiac and respiratory fluctuations) and scanner drift, it was included as a nuisance signal to minimize the influence of such factors (Gavrilescu et al. 2002; Macey et al. 2004; Birn et al. 2006). In order to extract the nuisance covariate time series for WM and CSF, we 1st segmented each individual's high-resolution structural image, using FSL's FAST segmentation program. The resulting segmented WM and CSF images were then thresholded to ensure 80% tissue type probability. These thresholded masks were then applied to each individual's time series, and a mean time series was calculated by averaging across all voxels within the mask (for individual examples of WM and CSF masks and placement, see Supplementary Fig. 3).

Functional Connectivity: Statistical Analysis

For each hemisphere, a multiple regression analysis was performed for each individual subject (using the general linear model implemented in FSL's FEAT), including the time series for the 6 basal ganglia seeds and the 9 nuisance covariates as predictors.

Time series for the basal ganglia seeds were orthogonalized (using the Gram-Schmidt process) with respect to each other, and with respect to the nuisance covariates, to ensure that the time series for each seed mask reflected its unique variance. This analysis produced individual subject-level maps of all positively and negatively predicted voxels for each regressor. As shown in Margulies et al. (2007), orthogonalizing the time series for each of the seeds with respect to each other does not lead to underestimation of functional connectivity due to removal of common variation, or artifactual generation of negative correlations (see Supplementary Fig. 4).

Group-level analyses were carried out using a mixed-effects model (FLAME) implemented in FSL. Corrections for multiple comparisons were carried out at the cluster level using Gaussian random field theory (min $Z > 3.1$; cluster significance: $P < 0.01$, corrected). This group-level analysis produced threshold Z score maps of activity associated with each basal ganglia seed as well as direct comparison of functional connectivity between striatal seeds. For a summary sketch of data path, see Figure 2.

Results

Positive Relationships

Inferior and Superior Ventral Striatum

Examination of functional connectivity during rest revealed a differential pattern of OFC connectivity among ventral striatum subregions (see Fig. 3 and Table 2). More specifically, spontaneous fluctuations in the VSi seed, which was selected to approximate the location of the nucleus accumbens, primarily correlated with the medial OFC (Brodmann area [BA] 11/25), whereas the VSs seed predicted patterns of activity in more superior and lateral portions of OFC (BA 10). This pattern of distinct regional functional differentiation between neighboring ventral striatal seeds extended beyond OFC. Specifically, VSi predicted activation within regions implicated in emotional

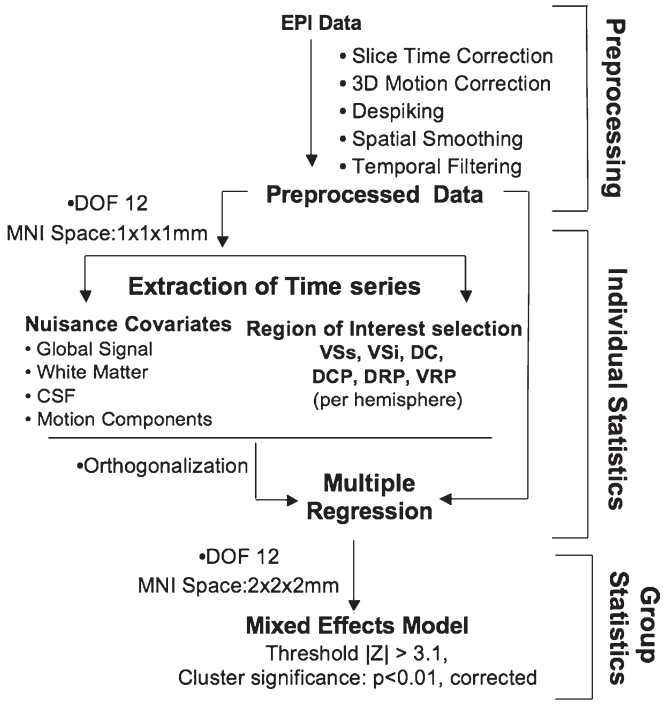

Figure 2. Data analysis overview. Summary sketch of the data analysis steps included in preprocessing, and individual and group statistics. Abbreviations from the top: DOF- degrees of freedom.

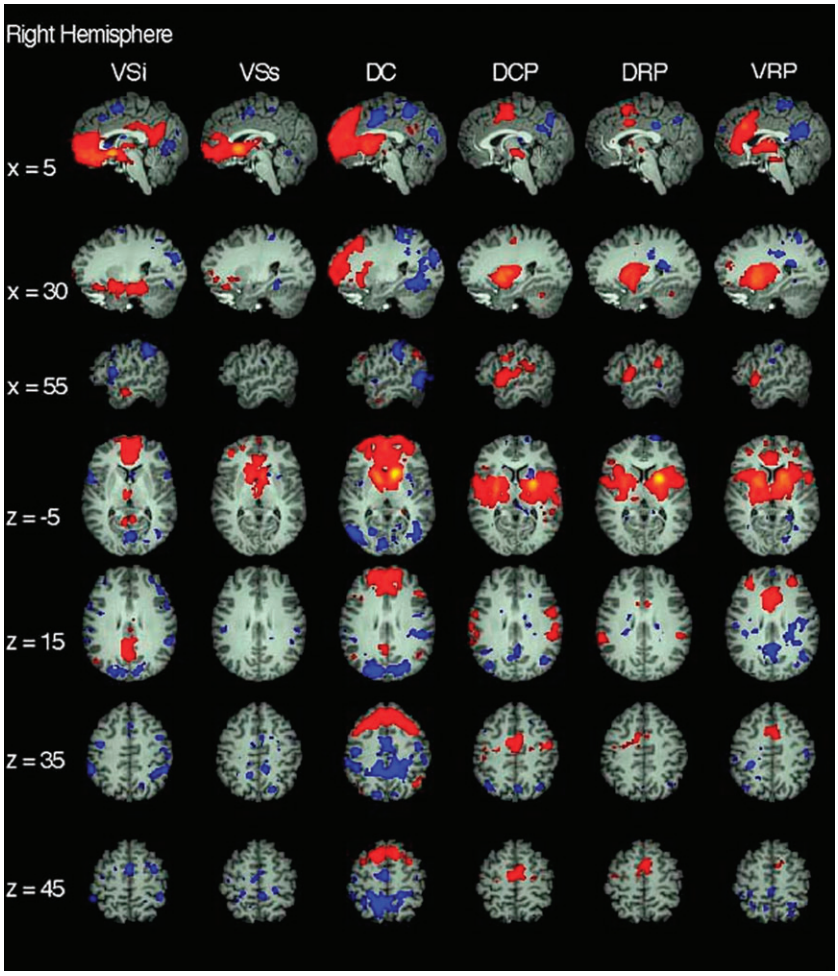

Figure 3. Functional connectivity of right hemisphere striatal seeds. Pattern of significantly positive (red) and negative (blue) relationships for right VSi ($x = 9$, $y = 9$, $z = -8$), VSs ($x = 10$, $y = 15$, $z = 0$), DC ($x = 13$, $y = 15$, $z = 9$), DCP ($x = 28$, $y = 1$, $z = 3$), DRP ($x = 25$, $y = 8$, $z = 6$), and VRP ($x = 20$, $y = 12$, $z = -3$), from left to right columns, respectively (Z score $> |3.1|$, cluster significance: $P < 0.01$, corrected). The 1st 3 rows are sagittal views (at $x = 5$, 30, and 55 from top to bottom, respectively), the last 4 rows are axial views (at $z = -5$, 15, 35, 45 from top to bottom, respectively). See text for details.

processing such as parahippocampal gyrus, and posterior cingulate cortex (BA 23), whereas VSs did not. In contrast, the VSs seed predicted activity in regions associated with executive function, decision making, and motor planning such as dorsolateral prefrontal cortex (DLPFC; BA 9), inferior frontal gyrus (BA 47), and rostral anterior cingulate (BA 32). Such differences were supported by the direct statistical comparisons between VSs and VSi seeds (see Fig. 4 and Table 3 for direct comparisons of the right hemisphere seed).

Though present in both hemispheres, the VSs relationships described above were more extensive for the left hemisphere. Otherwise, no substantial hemispheric differences were noted for the VSi and VSs seeds (see Supplementary Fig. 5 and Supplementary Tables 1 and 2).

Dorsal Caudate

Consistent with models emphasizing the involvement of dorsal caudate in cognitive control (Alexander et al. 1986; Cavada and Goldman-Rakic 1991; Parent and Hazrati 1995), the dorsal caudate predicted activity bilaterally in DLPFC, ventral lateral prefrontal cortex (BA 47), ACC (BA 32), and parietal association areas (inferior parietal lobule, BA 40). Furthermore, the dorsal caudate seed predicted activity in the frontal eye field (BA 8), supporting its location within the oculomotor loop described by Alexander et al. (1986). Unlike the more inferior ventral striatal seeds, the dorsal caudate seed did not display connectivity with limbic circuits implicated in affective processes (see Fig. 3 and Table 2). When compared directly with VSi, the dorsal caudate seed was more highly correlated with the aforementioned regions implicated in cognitive control, as opposed to the greater correlations found between VSi and ventral medial prefrontal, cingulate cortices, and limbic regions (see Fig. 4 and Table 4). The direct comparison of DC versus VSs showed greater correlation of DC with dorsal lateral prefrontal regions (see Fig. 4 and Table 4). There were no relevant hemispheric differences with respect to the DC seed (see Supplementary Tables 2 and 3).

Putamen

In contrast to the pattern of results observed among the caudate seeds, the putamen seeds predicted activity in primary and secondary cortical motor areas, as supported by direct statistical comparison when we combined the 3 caudate seeds (VSi, VSs, DC) versus the 3 putamen seeds (DCP, DRP, VRP) combined (see Supplementary Fig. 6 as well as Table 5 and Supplementary Table 4 for the right and left seeds, respectively).

Table 2
Positive relationships of right striatal and dorsal caudate seeds

Seed	Region	BA	Talairach			*Z*
			x	*y*	*z*	
VSi						
	OFC/ACC (L)	25/11	−8	27	−13	8.73
		11	−4	54	−11	7.22
	Inferior frontal gyrus (R)	47/13	32	13	−12	6.04
		47	28	26	−20	5.87
	Precuneus (L)	7	−6	−60	34	5.09
	Posterior cingulate (L)	23	−6	−56	17	5.52
		23	−6	−24	31	4.27
		24	−4	11	27	3.75
	Parahippocampal gyrus		−26	−20	−12	5.79
			18	−18	−14	6.50
	Inferior/middle temporal gyrus (R and L)	21	48	4	−34	5.57
		21	−60	−10	−13	5.12
		20	54	−7	−16	6.11
	Caudate head (L)		−10	7	−7	9.87
VSs						
	Medial frontal gyrus (C)	10	0	64	0	5.77
	Anterior cingulate gyrus (R)	32	2	43	−4	5.50
	Caudate head (L)		−10	10	0	8.62
DC						
	Superior frontal gyrus (R and L)	9	22	47	36	6.71
		9	−16	54	29	6.00
		10	20	67	−8	6.05
		10	30	62	5	5.81
		10	−32	56	−3	4.87
		8	14	30	48	6.02
		8	−20	24	47	5.66
		11	−22	56	−10	4.87
	Middle frontal gyrus (R and L)	8	36	24	45	5.21
		8	−46	14	40	5.30
	Middle/inferior frontal gyrus (L)	45	−30	27	41	5.42
	Inferior frontal gyrus (L)	47	28	15	−14	3.36
	Medial frontal gyrus (R and L)	10	2	63	15	6.14
		10	−2	53	5	6.32
		9	0	48	31	5.89
	Anterior cingulate (R)	32	14	36	11	5.14
		32	2	40	13	6.13
	Posterior cingulate (R)	31	−4	−49	30	3.79
	Inferior parietal lobule (L)	40	50	−58	43	5.27
	Inferior/middle temporal gyrus (R and L)	20	66	−26	−14	4.54
		21	−64	−26	−14	4.54
		21	54	−9	−28	3.92

Note: List of the brain regions showing a significant ($|Z| > 3.1$; cluster significance: $P < 0.01$, corrected) positive relationship with VSi ($x = 9$, $y = 9$, $z = -8$), VSs ($x = 10$, $y = 15$, $z = 0$), and DC ($x = 13$, $y = 15$, $z = 9$) in the right hemisphere seeds. L: left; R: right; *Z*: *Z* score of peak of activation.

This finding is consistent with the known involvement of putamen in motor function. In addition, the putamen seeds predicted activity in areas linked to executive control, such as DLPFC and rostral ACC.

Dorsal Caudal Putamen and Dorsal Rostral Putamen

The right DCP seed positively correlated with sensori-motor areas including primary and supplementary motor cortex (BA 4 and BA 6), and caudal ACC (BA 32 and BA 24). Similarly, the right dorsal rostral putamen seed predicted activity within secondary motor areas such as supplementary motor areas (BA 6) and ACC (BA 32 and 24) (see Fig. 3 and Table 6). Direct comparisons of DCP versus DRP showed greater correlations between DCP and premotor cortices (BA 6) in the right hemisphere (left hemisphere differences were subthreshold); DRP had greater correlation with dorsal ACC when compared with DCP in the left hemisphere (right hemisphere differences were subthreshold) (see Table 7 and Supplementary Table 5 for direct comparisons of the right and left seeds, respectively). Beside the aforementioned differences, there were no substantial differences between the right and left seeds (see Supplementary Fig. 5 and Supplementary Table 6 for positive relationships with the left hemisphere seeds).

Ventral Rostral Putamen

The ventral rostral putamen seed positively correlated with rostral portions of ACC (BA 32 and BA 24) and DLPFC (BA 10) commonly associated with conflict monitoring and error-related processes (Carter et al. 1998; van Veen et al. 2001; Bush et al. 2002; Botvinick et al. 2004; Ullsperger and von Cramon 2004) (see Fig. 3 and Table 6). Further, the ventral rostral seed predicted activation of insula cortex (BA 13). Results from the direct comparisons between the ventral rostral and the 2 dorsal putamenal seeds supported the greater correlation of the DLPFC and rostral ACC with the ventral rostral putamen (see Table 7 and Supplementary Fig. 7). With the exception of a positive relationship with the anterior lobule of the cerebellar vermis (culmen, lobule V) for the left but not the right ventral rostral seed, there were no substantial laterality differences between the putamen seeds (see Supplementary Tables 5 and 6).

Negative Relationships

We observed a number of networks negatively correlated with our basal ganglia seeds. In other words, increases in a seed region's activity predicted decreases in the negatively related region's activity. Interestingly, as depicted in Figure 5, caudate seeds were negatively correlated with some of the same areas that were positively related to the putamen seeds (e.g., supplementary and primary motor areas, and portions of dorsal ACC). Similarly, the putamen seeds were negatively correlated with some of the same areas that were positively correlated with the caudate seeds (e.g., ventromedial prefrontal cortex, precuneus). Such a distinction in connectivity between putamen and caudate seeds mirrors the differential roles in motor and affective processing commonly attributed to these regions.

Ventral Striatum and Dorsal Caudate

Ventral striatal regions (VSi and VSs) exhibited a distributed pattern of negative relationships with superior parietal regions commonly associated with spatial and temporal attentional selection (Fernandez-Duque et al. 2000; Coull et al. 2003; Nobre et al. 2004; Lepsien and Nobre 2006), occipital cortices and portions of the superior temporal, dorsolateral prefrontal cortices associated with cognitive control (Badgaiyan 2000; Banich et al. 2000; MacDonald et al. 2000; Casey et al. 2000; Andres 2003; Milham et al. 2003). Results corresponding to the right hemisphere seeds are shown in Figure 3 and Table 8. In contrast to VSi, DC showed greater negative correlations with precuneus, posterior cingulate, occipital cortices, and the cerebellar culmen. The differences in the pattern of negative correlations between VSs and VSi did not remain significant after full brain statistical correction. The pattern of negative relationships in the VSi, VSs, and dorsal caudate was not substantially different in the left hemisphere seeds (see Supplementary Fig, 5 and Supplementary Table 7).

Putamen

All 3 putamen seeds were negatively related with posterior medial default-mode network regions that were positively correlated with the inferior ventral striatal seed (e.g.,

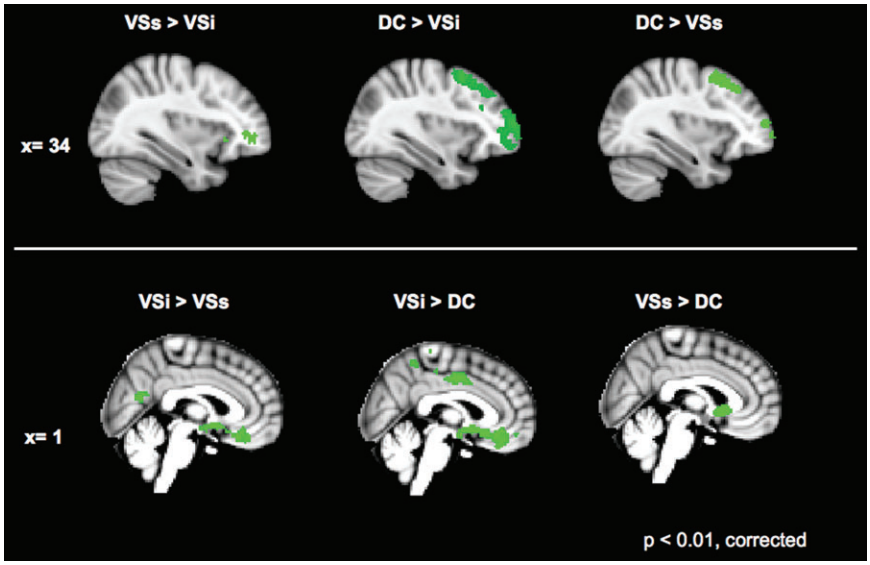

Figure 4. Direct comparisons for caudate seeds. The 1st 2 columns depict comparisons of the VSi with DC and VSs. The 3rd column represents the comparison between DC and VSs. The top row shows the regions in which the 1st seed has significantly greater positive correlations than the 2nd seed tested at $x = 34$. The lower row shows the reverse comparisons at $x = 0$. Z score $> |3.1|$; cluster significance: $P < 0.01$, corrected. See text for details.

posterior cingulate cortex and precuneus); see Figure 3 and Table 9 for the right hemisphere seed negative relationships. Although this pattern was qualitatively strongest for the ventral rostral putamen seed, the 3 putamen seeds did not differ significantly from each other. There were no substantial hemispheric differences with respect to putamen negative relationships (see Supplementary Fig. 5 and Supplementary Table 8 for the left hemisphere seed negative relationships).

Discussion

This resting state study of 35 healthy individuals provides a comprehensive examination of functional connectivity of the human striatum, revealing distinct neural circuits associated with each of the 6 striatal subregions we examined. Our results are consistent with a recent meta-analysis of 126 task-based functional studies (Postuma and Dagher 2006) while confirming the existence of hypothesized relationships between ventral striatum seeds and OFC, which could not be discerned in the meta-analysis. As hypothesized, our findings highlight the intimate relationship between ventral striatum and OFC, suggesting a potential differentiation in OFC connectivity between superior and inferior portions of the ventral striatum. Specifically, although the most inferior seed (VSi), placed in the proximity of nucleus accumbens, was primarily associated with medial portions of OFC, the intermediately placed VSs seed was associated with more lateral portions of OFC. These findings are in agreement with the nonhuman primate literature showing that medial OFC areas project to ventromedial limbic striatal areas, whereas lateral OFC components project to more dorsolateral parts of the striatum (Ferry et al. 2000). In addition, these data are consistent with human fMRI studies demonstrating that medial and lateral OFC functions are dissociable (Elliott et al. 2000a).

Consistent with models positing a cognitive/affective division between dorsal and ventral striatum (Selemon and Goldman-Rakic 1985; O'Doherty et al. 2004; Reiss et al. 2005), we found a dorsal/ventral distinction in caudate connectivity, though with a more gradual transition than previously appreciated in human studies. Specifically, although the most dorsal caudate seed was primarily associated with DLPFC and other cognitive control regions, and the most inferior caudate seed (VSi) was primarily associated with limbic areas, the intermediate seed (VSs) was associated with both cognitive control and limbic areas. Thus, at the macro-level of analysis observable with fMRI, our data are consistent with models positing that information is transferred along a ventral to dorsal gradient via circuits that spiral from emotional/motivational areas to decision making/executive control areas and then to motor control areas (Haber et al. 2000; Haber 2003).

As predicted by models positing the existence of motor and cognitive/association subdivisions of putamen (Parent and Hazrati 1995), as well as the findings of Postuma and Dagher (2006), we also found evidence for a putamenal rostral/caudal distinction. The 2 caudal putamen seeds were significantly correlated with primary and supplementary motor cortices, whereas the rostral putamen seed revealed patterns of connectivity with frontal regions implicated in executive function control. Our data also provide support for Postuma and Dagher's (2006) finding of putamen connectivity with the insula, specifically in the ventral rostral putamen.

Similar to our examination of ACC subregions (Margulies et al. 2007), we also found strongly negative as well as positive correlations with distinct antiphase networks for each striatal seed region. That is, the spontaneous signal fluctuations in such negatively correlated networks are 180° out of phase with the fluctuations observed in the corresponding seed region. Although the significance of such antiphase relationships remains unclear, a defensible generalization seems to be that they arise between functional systems with apparently opposite goals or functions (Greicius et al. 2003; Fox et al. 2005; Margulies et al. 2007; Fransson 2005; Kelly et al. 2008). Consistent with this

Table 3
Direct comparisons: right VSs versus VSi

Contrast	Region	BA	Talairach			Z
			x	y	z	
VSi > VSs						
	OFC (R)	11/25	8	27	−15	4.25
	Rectal gyrus (L)	11	−10	34	−19	4.02
	Anterior cingulate (R)	25	6	7	−7	8.81
	Parahippocampal gyrus (R & L)	36	34	−28	−17	4.35
		36	30	−37	−8	3.87
		36	−30	−34	−10	5.39
		36	−44	−7	−13	3.50
		35	20	−26	−14	5.00
		35	−20	−22	−16	4.34
		27	10	−37	−2	4.30
	Parahippocampal gyrus/amygdala (L)		−26	−1	−17	4.82
	Precuneus/posterior cingulate (C)	23	0	−59	20	4.25
	Culmen (R)		20	−40	−17	4.67
	Putamen (L)		−14	5	−10	6.18
VSs > VSi						
	Inferior/middle frontal gyrus (L)	46/10	−42	47	1	4.59
	Thalamus (L)		−2	−7	13	4.81
	Caudate (L)		−8	16	3	6.93

Note: List of the brain regions resulting significantly correlated with right VSi and VSs when the 2 seeds were directly compared. ($|Z| > 3.1$; cluster significance: $P < 0.01$, corrected). R: Right; L: Left; *Z*: *Z* score of peak of activation.

notion, spontaneous fluctuations in seed regions implicated in affective processing (e.g., VSi) were generally in antiphase relationship with fluctuations in regions involved in cognitive and/or motor control. Recent work in our lab suggests that such antiphase relationships may be functionally significant. For example, Kelly et al. (2008) showed that individual differences in behavioral variability during a flanker task were strongly correlated with individual differences in the magnitude of the coupling of the antiphase relationships between the default-mode network and its anticorrelated frontal–parietal task-positive network (whether observed during rest or task performance). The mechanism by which negative correlations arise between networks is unclear (Fox et al. 2005; Fox and Raichle 2007). It is possible that they may reflect antagonistic influences of one network on another, as suggested by granger causality analyses in a recent study of the default-mode network and its antinetworks in our laboratory (Uddin et al. forthcoming). Further exploration of striatal antiphase networks and the possible contributions of compromises in these relationships to behavior, including psychopathology, is merited.

Our cortical–striatal results are fully consistent with estimations of human connectivity from macaque anatomic studies. Specifically, our data are consistent with all 5 classical cortical–striatal loops (Alexander et al. 1986). We found that dorsal putamen is correlated with primary motor and somatosensory cortex and supplementary motor area (Kunzle 1975; Kunzle 1977); that dorsal caudate is correlated with DLPFC (Selemon and Goldman-Rakic 1985; Middleton and Strick 2002; Kelly and Strick 2004), and the frontal eye fields (Kunzle and Akert 1977); that VSs, which is approximately equivalent to ventromedial caudate, is functionally connected to lateral orbitofrontal regions (Ilinsky et al. 1985; Selemon and Goldman-Rakic 1985; Ferry et al. 2000; Haber et al. 2006); and that VSi is significantly correlated with ACC (Powell and Leman 1976; Yeterian and Van Hoesen 1978; Selemon and Goldman-Rakic 1985; Ferry et al. 2000; Haber et al. 1995; Haber et al. 2006). Of note, most of our findings appear to be bilateral, regardless

Table 4
Direct comparisons: right DC versus right VSi and versus right VSs

Contrast	Region	BA	Talairach			Z
			x	y	z	
DC > VSi						
	Superior frontal gyrus (R and L)	8	16	32	52	5.46
		8	−8	51	38	5.24
		8	20	43	38	4.75
		10	16	56	19	5.30
		10	30	62	−3	4.93
		10	−34	56	−3	4.98
		10	−22	52	20	4.88
		6	−20	26	54	5.09
	Middle/superior frontal gyrus (R)	6	34	14	49	5.73
	Middle frontal gyrus (R and L)	9	42	31	33	5.14
		9	−44	27	37	5.53
		10	32	57	8	5.09
		10	22	67	8	4.86
		10	38	44	−9	4.27
		10	−40	50	−14	4.22
		4	−48	12	40	5.30
		46	46	32	20	5.36
		8	−34	14	53	4.74
	Inferior frontal gyrus (R and L)	45	54	20	12	4.63
	Medial frontal gyrus (C and R and L)	8	2	27	41	5.54
		9	0	49	36	5.35
		9	−2	56	19	4.00
	Inferior parietal lobule (R and L)	40	50	−58	43	4.29
		40	−58	−53	41	4.80
	Caudate (L)		−14	14	7	7.50
VSi > DC						
	Middle frontal gyrus (R)	11	26	35	−12	3.81
	Rectal gyrus (R)	11	6	34	−20	4.81
	Insula (R)	13	38	9	−7	4.02
	Anterior cingulate (R and L)	25	6	9	−7	10.15
		32	6	48	−14	4.01
		32	−10	36	−15	5.39
	Cingulate gyrus (R and L)	24	6	−16	39	4.62
		24	−6	−6	37	4.78
	Posterior cingulate (R and L)	30	6	−39	2	4.17
	Parahippocampal gyrus (R and L)	28	20	−18	−14	5.29
		28	−24	−22	−12	4.53
		36	−24	−43	−11	4.20
		36	−34	−32	−22	4.73
	Uncus (R and L)	28	22	−5	−30	4.10
		20	−28	2	−30	4.82
	Lingual gyrus (R)	19	10	−51	3	4.23
	Amygdala (L)		−28	−1	−15	5.10
	Thalamus (L)		−10	7	−9	6.53
	Declive (L)		−32	−59	−14	4.21
	Culmen (L)		−38	−42	−21	4.24
DC > VSs						
	Superior frontal gyrus (R and L)	10	20	67	10	5.60
		10	30	62	−3	4.28
		9	4	50	31	5.34
		8	−16	28	48	4.49
		6	−4	20	54	4.14
	Middle frontal gyrus (R and L)	8	34	33	39	5.22
		8	−42	27	35	3.92
		9	−48	15	36	4.46
		9	−20	54	27	5.34
		9	42	16	40	5.03
	Medial frontal gyrus (L)	10	−2	53	5	5.15
		8	−6	45	40	5.35
	Supramarginal gyrus (R)	40	52	−53	32	4.89
	Anterior cingulate (L)	32	−12	37	7	3.68
	Thalamus (L)		−14	−17	17	4.61
	Caudate (L)		−14	3	13	13.70

Note: List of the brain regions resulting significantly correlated with right DC, Vsi, or VSs when these seeds were directly compared VSs > DC comparison resulted in no differences with this statistical threshold. ($|Z| > 3.1$; cluster significance $P < 0.01$, corrected). R: Right; L: Left; *Z*: *Z* score of peak of activation.

of the hemisphere seeded. Although there has been some controversy in the literature about direct contralateral anatomical thalamic projections (DeVito and Anderson 1982; Fenelon et al. 1990; Parent et al. 1999), contralateral

Table 5
Direct comparisons: right caudate versus putamen

Contrast	Region	BA	Talairach			*Z*
			x	*y*	*z*	
Caudate > putamen						
	Superior frontal gyrus (R and L)	10	12	66	0	6.79
		10	−22	66	−1	5.86
		10	−18	63	15	5.59
		8	22	29	43	4.87
		8	−20	37	39	4.45
		9	18	43	38	4.37
	Middle frontal gyrus (R and L)	10	38	54	−13	5.32
		8	46	−11	−20	4.96
		8	−30	27	43	4.79
		8	−24	25	34	4.83
		10	−38	56	−5	4.71
		9	−2	42	−17	6.74
	Inferior frontal gyrus (R)	11	26	26	−20	4.68
	Medial frontal gyrus (R and L)	6	12	31	35	4.38
		9	6	44	14	5.03
		9	−6	52	−18	6.64
		10	−12	42	−14	6.39
		10	−2	63	2	6.91
		9	−20	37	29	4.35
	Inferior parietal lobule (L)	39	−44	−66	42	5.83
	Precuneus (C)	7	0	−62	40	5.35
	Anterior cingulate gyrus (L)	32	−10	29	−13	6.59
	Posterior cingulate gyrus (C and R)	31	0	−33	35	5.97
		29	4	−52	15	4.85
	Middle temporal gyrus (R and L)	21	58	−3	−23	6.01
		21	−68	−28	−10	5.11
		20	−48	−5	−23	5.00
		42	−64	−10	−13	5.81
	Inferior temporal gyrus (R)	20	54	−22	−16	5.44
	Parahippocampal gyrus (R)		36	−18	−16	4.59
	Angular gyrus (R and L)	39	48	−66	36	5.44
		39	−48	−67	31	5.76
	Caudate (R and L)		6	14	−2	
			−6	8	−4	7.61
			−10	18	−1	7.53
Putamen > caudate						
	Precentral gyrus (R and L)	6	44	−8	37	5.65
		6	−42	−8	41	5.63
	Inferior frontal gyrus (R and L)	9	44	3	29	5.64
		46	46	35	0	5.04
		45	−52	28	6	4.15
	Medial frontal gyrus (R and L)	6	14	−3	61	5.44
		6	−6	−5	61	4.91
		8	−12	−29	44	5.05
	Insula (R and L)	13	−46	12	−4	7.17
	Inferior parietal lobule (R and L)	40	60	−32	24	6.01
		40	−66	−37	31	6.13
		40	−64	−24	23	6.26
	Anterior cingulate gyrus (R and L)	32	6	10	40	6.43
		24	−10	4	42	6.72
	Superior temporal gyrus (R and L)	22	54	8	0	7.10
		22	−66	−34	20	5.97
		22	−60	0	4	6.20
	Thalamus (R)		10	−23	1	6.37
	Declive (R and L)		16	−59	−11	4.41
			−12	−73	−11	5.36
	Putamen (R and L)		18	12	−2	12.66
			−30	−13	4	8.14
			−28	6	3	8.01

Note: List of the brain regions resulting significantly correlated with the right caudate seeds combined (VSi + VSs + dorsal caudate) and the right putamen seeds combined (DCP + DRP + VRP) when these were directly compared. ($|Z| > 3.1$; cluster significance $P < 0.01$, corrected). R: Right; L: Left; *Z*: *Z* score of peak of activation.

Table 6
Positive relationships of right putamen seeds

Seed	Region	BA	Talairach			*Z*
			x	*y*	*z*	
DCP						
	Precentral gyrus (R and L)	6	−50	−9	50	3.77
		6	−52	−6	6	5.17
		4	48	−6	43	5.06
		4	−48	−10	36	4.66
		4	−30	−15	50	3.72
	Postcentral gyrus (L)	40	−60	−19	18	5.90
	Anterior cingulate gyrus (R and L)	24	10	0	44	4.96
		32	4	10	42	5.29
		32	−6	8	46	6.03
	Superior temporal gyrus (R and L)	22	50	2	2	6.84
		22	−64	−40	17	4.17
	Middle temporal gyrus (L)	37	−48	−50	4	4.87
	Lentiform nucleus (L)		−28	−8	6	8.69
	Thalamus (L)		−12	−21	1	6.27
DRP						
	Superior frontal gyrus (R)	6	4	11	57	4.91
	Middle frontal gyrus (L)	6	−32	−5	46	3.62
	Inferior parietal lobule (R and L)	40	−58	−36	24	4.90
		40	52	−30	25	4.08
	Superior temporal gyrus (L)	22	−56	8	1	4.89
	Anterior cingulate gyrus (R and L)	24	4	9	33	4.88
		32	−8	11	34	4.68
	Lentiform nucleus (L)		−30	−2	7	6.95
			−28	0	−8	6.79
	Thalamus (L)		−6	−14	−1	4.04
VRP						
	Superior frontal gyrus (R)	10	28	46	23	4.98
		6	20	15	58	4.44
	Precentral gyrus (L)	44	−62	8	10	3.07
	Middle frontal gyrus (R and L)	10	−34	42	22	4.74
		10	38	47	11	3.92
		11	−28	46	−11	3.83
	Insula (R and L)	13	−44	12	3	6.72
		13	44	14	−2	5.72
	Anterior cingulate gyrus (R and L)	32	2	25	30	7.48
		24	−6	35	7	5.58
	Lentiform nucleus (L)		−20	4	11	8.60
			−20	12	−4	8.32

Note: List of the brain regions showing a significant ($|Z| > 3.1$; cluster significance $P < 0.01$, corrected) positive relationship with the right DCP ($x = 28$, $y = 1$, $z = 3$), DRP ($x = 25$, $y = 8$, $z = 6$), and VRP seeds ($x = 20$, $y = 12$, $z = -3$). L: left; R: right; *Z*: *Z* score of peak of activation.

corticostriatal anatomical connections have been described in primates (Arikuni and Kubota 1986) and in a DTI study in humans (Lehericy et al. 2004). Our findings of bilaterality agree with the pattern of striatal coactivation described by Postuma and Dagher (2006). However, they are functional correlations and do not necessarily reflect direct WM connectivity. Ongoing studies combining DTI and functional connectivity fMRI will clarify whether such correlational patterns are supported by direct anatomical connections.

These data provide a framework for the examination of functional connectivity in various clinical disorders. The correlation of the VSi with medial aspects of OFC is of particular clinical interest given the implication of this OFC area (BA 25) in affect regulation and substance abuse. For example, BA 25 is overactive in treatment resistant depression which may be reduced by chronic deep brain stimulation in that location (Mayberg et al. 2005). Volkow et al. (2006) found that nonalcoholic relatives of alcoholics have increased availability of D2 receptors in the ventral striatum and that higher levels of D2 receptors in striatum correlate positively with higher metabolic activity in OFC and ACC, including BA 25. Given the role of both VS and OFC in reward processing (Rolls 2000; Elliott et al. 2000b; Schultz et al. 2000), straightforward quantification of the connectivity of this circuit can increase our understanding of clinical conditions associated with dysregulation of reward mechanisms, such as depression, substance abuse, and ADHD (Epstein et al. 2006; Forbes et al. 2006; Chang et al. 2007; Scheres et al. 2007).

This study has several limitations. First, we only examined functional connectivity during resting state, and the amplitude of resting state network fluctuations is modulated by the transition between task performance and rest (e.g., Fransson 2005; DeLuca et al. 2006; Sridharan et al. 2007). Although the spatiotemporal stability of resting state functional networks is impressive (Damoiseaux et al. 2006), future studies should examine task-related changes in the connectivity of basal ganglia circuits. Second, we limited our analyses to 6 striatal subregions due to the spatial resolution limits on our data acquisition. Future work using higher resolution fMRI will examine the connectivity of other basal ganglia subregions (i.e., globus pallidus internal/external segments, substantia nigra, and thalamic nuclei). Incomplete coverage of the inferior portions of cerebellum prevented us from fully appreciating striatal-cerebellar functional interactions which were observed for superior regions of the cerebellum. Another type of limitation is our lack of understanding of the neuronal and vascular substrates that underlie the remarkable patterns of low frequency temporal coherence (Biswal et al. 1995) which provide the bases for functional connectivity maps (Fox and Raichle 2007). The absence of a plausible model has led to skepticism regarding this approach (Morcom and Fletcher 2006), despite accumulating evidence that it is a robust (Buckner and Carroll 2007), stable (Damoiseaux et al. 2006) and intriguingly revealing technique (Margulies et al. 2007). Finally, similar to prior studies, the present work detected a number of robust negative relationships in spontaneous activity among neural systems with seemingly competing functions. Although intriguing, one concern that arises is the possible contributions of analytical procedures, such as global normalization or orthogonalization, to the presence of such relationships. However, prior work has demonstrated that antiphasic relationships can not be simply attributed to correction for the global signal (Fransson 2005; Uddin et al. forthcoming). Similarly, Margulies et al. (2007) and the present work demonstrated that analytical decisions such as simultaneous regression of multiple seed regions in a single model or orthogonalization are not responsible for detection of such relationships either (see Supplementary Fig. 4). As such, these negative relationships do not appear artifactual in nature and merit future study to elucidate their significance (see Kelly et al. 2008 for an initial effort). In summary, the present work demonstrates the promise of resting state approaches for comprehensively examining basal ganglia circuitry. In a single study during rest lasting less then 7 min per subject, we demonstrated differential patterns of connectivity among 6 striatal subregions along an affective/cognitive/motor axis predicted by contemporary models of basal ganglia function (Middleton and Strick 2000a; Haber 2003), with higher degree of specificity than previously appreciated by a meta-analysis of over 100 human neuroimaging studies. The cost-effectiveness

Table 7
Right direct comparisons: putamen seeds

Contrast	Region	BA	Talairach			Z
			x	y	z	
VRP > (DCP + DRP)						
	Superior frontal gyrus (R)	10	14	64	0	4.18
	Middle frontal gyrus (R)	10	34	52	−9	3.93
	Medial frontal gyrus (R and L)	10	18	51	7	4.39
		10	−10	59	3	5.01
	Anterior cingulate (R and L)	32	8	42	−9	4.67
		32	−8	28	23	4.68
		32	8	27	28	5.07
		24	−8	37	6	4.58
		24	−2	22	14	4.28
	Putamen (L)		−18	11	−9	7.28
(DCP + DRP) > VRP						
	Superior frontal gyrus (R)	6	14	−12	65	3.61
	Precentral gyrus (R and L)	6	54	0	30	4.98
		6	44	−10	37	4.36
		4	58	−18	40	4.66
	Medial frontal gyrus (R and L)	6	4	−3	54	4.87
		6	−2	−13	60	4.67
	Postcentral gyrus (R and L)	43	64	−17	14	4.71
		3	−54	−18	25	4.34
		8	−46	−19	45	4.86
	Anterior cingulate gyrus (L)	24	−10	−3	48	4.26
	Superior temporal gyrus (R)	22	58	−36	13	3.59
	Middle temporal gyrus (R)	46	50	−54	6	4.73
	Transverse temporal gyrus (L)	41	−38	−23	12	4.98
	Putamen (R and L)		26	6	5	8.64
			28	−15	4	4.98
			−32	−14	1	4.09
DCP > DRP						
	Precentral gyrus (R)	6	59	−2	28	4.42
		6	54	−2	12	3.67

Note: List of the brain regions resulting significantly correlated with the right VRP and the 2 right dorsal putamen seeds combined (DCP + DRP) when these seeds were directly compared. The DRP > DCP comparisons resulted in no differences at this statistical threshold. ($|Z| > 3.1$; cluster significance $P < 0.01$, corrected). R: right; L: left; *Z*: *Z* score of peak of activation.

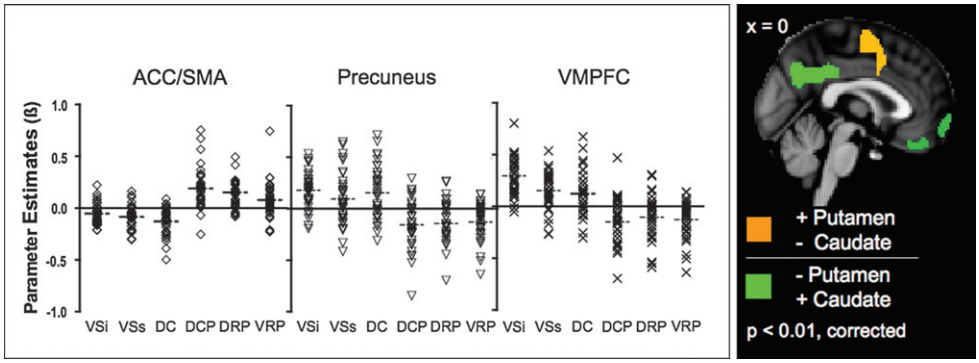

Figure 5. Brain regions correlated with both putamen and caudate but in opposite directions. On the left panel the scatter plots represent the mean parameter estimates (regression coefficients) of striatal seed connectivity (VSi, VSs, DC, DCP, DRP, and VRP, from left to right, respectively) with ACC/supplementary motor area (SMA), precuneus, and with ventromedial prefrontal cortex (VMPFC), from the left to right, respectively. Outlier β values not included in the scatter plot were as follow: $\beta = 1.07$ and -1.30 for DRP connectivity with ACC/SMA and precuneus, respectively; $\beta = -1.11$ for DCP connectivity with VMPFC. On the right panel the brain regions exhibiting positive correlations with the putamen seeds (i.e., DCP + DRP + VRP) but negative correlation with caudate seeds (i.e., VSi + VSs + DC) and vice versa (orange and green, respectively) are shown.

Table 8
Negative relationships of right striatal and dorsal caudate seeds

Seed	Region	BA	Talairach			Z
			x	y	z	
VSi						
	Superior frontal gyrus (R)	9	38	51	16	5.32
	Middle frontal gyrus (R and L)	46	46	38	20	4.86
		8	48	12	38	4.71
	Precentral gyrus (R)	6	−60	−17	43	4.60
		6	−46	−3	48	4.61
		6	−60	5	29	4.19
	Medial frontal gyrus	6	−4	1	57	4.02
	Inferior frontal gyrus (L)	45	58	13	21	5.85
		46	50	39	2	4.23
	Postcentral gyrus (R)	4	60	−17	43	4.60
	Supramarginal gyrus (L)	40	−62	−47	39	4.66
	Inferior parietal lobule (R)	40	64	−36	28	4.51
		40	52	−36	52	4.81
	Precuneus (R)	7	22	−63	34	4.66
	Middle temporal gyrus (L)	39	−46	−73	13	4.77
	Superior temporal gyrus (L)	22	−58	−38	15	4.18
	Cuneus (R and L)	17	−6	−89	8	4.11
		18	12	−87	23	5.09
		18	−2	−76	9	4.15
		18	−8	−88	28	4.50
	Lingual gyrus (L)	18	−14	−70	−3	4.10
		18	−28	−72	−5	3.85
	Cerebellar culmen (R)		10	−65	−5	4.45
VSs						
	Inferior frontal gyrus (R)	45	58	12	24	5.85
		46	50	40	4	4.23
		44	−60	12	6	4.69
	Middle frontal gyrus (R and L)	8	48	10	42	4.71
		10	38	52	20	5.32
	Precentral gyrus (L)	6	−46	−6	52	4.61
		6	−60	4	32	4.19
	Medial frontal gyrus (L)	6	−4	−2	62	4.03
	Inferior parietal lobule (R and L)	40	52	−40	54	4.81
		40	64	−38	28	4.51
		40	−62	−50	40	4.66
	Postcentral gyrus (R)	3	22	−30	66	4.33
		2	60	−20	46	4.60
	Precuneus (R)	7	22	−66	34	4.66
	Cuneus (R and L)	19	−28	−84	30	4.22
		18	12	−90	20	5.09
		19	−6	−92	4	4.11
	Lingual gyrus (L)	18	−8	−92	26	4.50
		18	−2	−78	6	4.15
		19	−28	−74	−10	3.85
	Cerebellar culmen (R)		10	−66	−10	4.45
DC						
	Precentral gyrus (R and L)	6	−44	−12	41	4.56
		6	32	−18	65	3.99
	Postcentral gyrus (L)	5	−56	−27	40	4.84
	Insula (L)	13	−38	0	6	3.69
	Inferior parietal lobule (R)	40	52	−30	33	4.79
		40	−66	−32	22	3.94
	Precuneus (R and L)	7	−20	−80	39	5.94
		7	12	−78	46	3.65
	Posterior cingulate	31	−8	−42	48	6.11
		31	16	−64	16	4.41
	Mid cingulate gyrus	24	−10	−8	35	4.68
		24	−2	4	37	5.05
	Anterior cingulate gyrus	32	−6	16	40	4.85
	Superior temporal gyrus (R)	22	58	−4	−4	4.98
	Middle temporal gyrus (R)	37	−48	−68	13	5.42
		39	42	−58	7	5.00
	Lingual gyrus (L)	18	−14	−72	−1	5.06
	Cuneus (R and L)	18	−22	−68	14	3.61
		19	−10	−78	32	6.12
		18	24	−82	32	4.59

Note: List of the brain regions showing a significant ($|Z| > 3.1$; cluster significance $P < 0.01$, corrected) negative relationship with the right VSi ($x = 9$, $y = 9$, $z = -8$), VSs ($x = 10$, $y = 15$, $z = 0$), and DC seeds ($x = 13$, $y = 15$, $z = 9$). L: left; R: right; *Z*: *Z* score of peak of activation.

combined with richly detailed results is an unique strength of resting state fMRI, which holds considerable promise for the study of basal ganglia circuitry dysfunction in clinical populations.

Table 9
Negative relationships of right putamen seeds

Seed	Region	BA	Talairach			Z
			x	y	z	
DCP						
	Superior frontal gyrus (R)	9	2	54	25	4.10
	Posterior cingulate (L)	31	−10	−45	34	3.61
	Precuneus	7/31	−8	−63	31	4.28
	Superior parietal lobule	7	−38	−64	51	4.06
	Inferior parietal lobule	40	−50	−60	44	4.18
	Angular gyrus (L)	39	−34	−74	31	4.13
	Putamen (R)		22	10	7	9.07
DRP						
	Inferior parietal lobule	40	34	−55	34	4.18
	Posterior cingulate gyrus (L)	31	2	−31	35	4.81
VRP						
	Medial frontal gyrus (R)	6	6	−26	66	3.92
	Precentral gyrus (R)	4	50	−14	38	4.52
		6	40	−6	26	4.32
		4	−18	−26	66	3.99
	Paracentral lobule (R)	5	4	−42	61	3.79
	Superior parietal lobule (L)	7	22	−59	62	4.05
	Postcentral gyrus (L)	3	−30	−31	48	5.66
		5	22	−36	63	4.32
	Precuneus (R and L)	7/31	6	−65	24	4.73
		7	−24	−52	51	4.46
	Posterior cingulate gyrus (L)	31	−4	−45	32	4.34
	Parahippocampal gyrus (L)	37	32	−43	−3	4.56

Note: List of the brain regions showing a significant ($|Z| > 3.1$; cluster significance $P < 0.01$, corrected) negative relationship with right DCP ($x = 28$, $y = 1$, $z = 3$), DRP ($x = 25$; $y = 8$, $z = 6$), and VRP seeds ($x = 20$, $y = 12$, $z = -3$). L: Left; R: Right; *Z*: *z* statistic of peak of activation.

Supplementary Material

Supplementary material can be found at: http://www.cercor.oxfordjournals.org/

Funding

Stavros S. Niarchos Foundation; and the National Alliance for Research on Schizophrenia and Depression.

Notes

We are sincerely grateful to the volunteers who participated in this study and wish to thank Dylan Gee for helpful editorial suggestions and 4 anonymous reviewers for their thoughtful comments. *Conflict of Interest*: None declared.

Address correspondence to Michael P. Milham, MD, PhD, Phyllis Green and Randolph Cōwen Institute for Pediatric Neuroscience, NYU Child Study Center, 215 Lexington Avenue, New York, NY 10016, USA. Email: milham01@med.nyu.edu.

References

Albin RL, Mink JW. 2006. Recent advances in Tourette syndrome research. Trends Neurosci. 29:175–182.

Alexander GE, DeLong MR, Strick PL. 1986. Parallel organization of functionally segregated circuits linking basal ganglia and cortex. Annu Rev Neurosci. 9:357–381.

Andres P. 2003. Frontal cortex as the central executive of working memory: time to revise our view. Cortex. 39:871–895.

Arikuni T, Kubota K. 1986. The organization of prefrontocaudate projections and their laminar origin in the macaque monkey: a retrograde study using HRP-gel. J Comp Neurol. 244:492–510.

Badgaiyan RD. 2000. Executive control, willed actions, and nonconscious processing. Hum Brain Mapp. 9:38–41.

Banich MT, Milham MP, Atchley RA, Cohen NJ, Webb A, Wszalek T, Kramer AF, Liang Z, Barad V, Gullett D, et al. 2000. Prefrontal

regions play a predominant role in imposing an attentional 'set': evidence from fMRI. Brain Res Cogn Brain Res. 10:1–9.
Beckmann CF, DeLuca M, Devlin JT, Smith SM. 2005. Investigations into resting-state connectivity using independent component analysis. Philos Trans R Soc Lond B Biol Sci. 360:1001–1013.
Bhatia KP, Marsden CD. 1994. The behavioural and motor consequences of focal lesions of the basal ganglia in man. Brain. 117(Pt 4): 859–876.
Birn RM, Diamond JB, Smith MA, Bandettini PA. 2006. Separating respiratory-variation-related fluctuations from neuronal-activity-related fluctuations in fMRI. Neuroimage. 31:1536–1548.
Biswal B, Yetkin FZ, Haughton VM, Hyde JS. 1995. Functional connectivity in the motor cortex of resting human brain using echo-planar MRI. Magn Reson Med. 34:537–541.
Botvinick MM, Cohen JD, Carter CS. 2004. Conflict monitoring and anterior cingulate cortex: an update. Trends Cogn Sci. 8: 539–546.
Braver TS, Barch DM, Gray JR, Molfese DL, Snyder A. 2001. Anterior cingulate cortex and response conflict: effects of frequency, inhibition and errors. Cereb Cortex. 11:825–836.
Brett M. 1999. The MNI brain and the Talaraich Atlas. Available at: http://www.mrc.cbu.cam.ac.uk/Imaging/mnispace.html. Accessed 19 December 1999.
Buckner RL, Carroll DC. 2007. Self-projection and the brain. Trends Cogn Sci. 11:49–57.
Bush G, Luu P, Posner MI. 2000. Cognitive and emotional influences in anterior cingulate cortex. Trends Cogn Sci. 4:215–222.
Bush G, Vogt BA, Holmes J, Dale AM, Greve D, Jenike MA, et al. 2002. Dorsal anterior cingulate cortex: a role in reward-based decision making. Proc Natl Acad Sci USA. 99:523–528.
Carter CS, Braver TS, Barch DM, Botvinick MM, Noll D, Cohen JD. 1998. Anterior cingulate cortex, error detection, and the online monitoring of performance. Science. 280:747–749.
Casey BJ, Thomas KM, Welsh TF, Badgaiyan RD, Eccard CH, Jennings JR, Crone EA. 2000. Dissociation of response conflict, attentional selection, and expectancy with functional magnetic resonance imaging. Proc Natl Acad Sci USA. 97:8728–8733.
Castellanos FX, Giedd JN, Marsh WL, Hamburger SD, Vaituzis AC, Dickstein DP, et al. 1996. Quantitative brain magnetic resonance imaging in attention-deficit hyperactivity disorder. Arch Gen Psychiatry. 53:607–616.
Cavada C, Goldman-Rakic PS. 1991. Topographic segregation of corticostriatal projections from posterior parietal subdivisions in the macaque monkey. Neuroscience. 42:683–696.
Chang L, Alicata D, Ernst T, Volkow N. 2007. Structural and metabolic brain changes in the striatum associated with methamphetamine abuse. Addiction. 102(Suppl. 1):16–32.
Coull JT, Walsh V, Frith CD, Nobre AC. 2003. Distinct neural substrates for visual search amongst spatial versus temporal distractors. Brain Res Cogn Brain Res. 17:368–379.
Crottaz-Herbette S, Anagnoson RT, Menon V. 2004. Modality effects in verbal working memory: differential prefrontal and parietal responses to auditory and visual stimuli. Neuroimage. 21:340–351.
Damoiseaux JS, Rombouts SA, Barkhof F, Scheltens P, Stam CJ, Smith SM, Beckmann CF. 2006. Consistent resting-state networks across healthy subjects. Proc Natl Acad Sci USA. 103:13848–13853.
Delgado MR. 2007. Reward-related responses in the human striatum. Ann N Y Acad Sci. 1104:70–88.
DeLuca M, Beckmann CF, De Stefano N, Matthews PM, Smith SM. 2006. fMRI resting state networks define distinct modes of long-distance interactions in the human brain. Neuroimage. 29:1359–1367.
DeVito JL, Anderson ME. 1982. An autoradiographic study of efferent connections of the globus pallidus in Macaca mulatta. Exp Brain Res. 46:107–117.
Dosenbach NU, Fair DA, Miezin FM, Cohen AL, Wenger KK, Dosenbach RA, Fox MD, Snyder AZ, Vincent JL, Raichle ME. 2007. Distinct brain networks for adaptive and stable task control in humans. Proc Natl Acad Sci USA. 104:11073–11078.
Drevets WC, Price JC, Kupfer DJ, Kinahan PE, Lopresti B, Holt D, et al. 1999. PET measures of amphetamine-induced dopamine release in ventral versus dorsal striatum. Neuropsychopharmacology. 21:694–709.
Elliott R, Dolan RJ, Frith CD. 2000a. Dissociable functions in the medial and lateral orbitofrontal cortex: evidence from human neuroimaging studies. Cereb Cortex. 10:308–317.
Elliott R, Friston KJ, Dolan RJ. 2000b. Dissociable neural responses in human reward systems. J Neurosci. 20:6159–6165.
Epstein J, Pan H, Kocsis JH, Yang Y, Butler T, Chusid J, Hochberg H, Murrough J, Strohmayer E, Stern E. 2006. Lack of ventral striatal response to positive stimuli in depressed versus normal subjects. Am J Psychiatry. 163:1784–1790.
Ernst M, Nelson EE, Jazbec S, McClure EB, Monk CS, Leibenluft E, Blair J, Pine DS. 2005. Amygdala and nucleus accumbens in responses to receipt and omission of gains in adults and adolescents. Neuroimage. 25:1279–1291.
Fair DA, Dosenbach NU, Church JA, Cohen AL, Brahmbhatt S, Miezin FM, Barch DM, Raichle ME, Petersen SE, Schlaggar BL. 2007. Development of distinct control networks through segregation and integration. Proc Natl Acad Sci USA. 104(33):13507–13512.
Fenelon G, Francois C, Percheron G, Yelnik J. 1990. Topographic distribution of pallidal neurons projecting to the thalamus in macaques. Brain Res. 520:27–35.
Fernandez-Duque D, Baird JA, Posner MI. 2000. Executive attention and metacognitive regulation. Conscious Cogn. 9:288–307.
Ferry AT, Ongur D, An X, Price JL. 2000. Prefrontal cortical projections to the striatum in macaque monkeys: evidence for an organization related to prefrontal networks. J Comp Neurol. 425: 447–470.
Forbes EE, Christopher MJ, Siegle GJ, Ladouceur CD, Ryan ND, Carter CS, Birmaher B, Axelson DA, Dahl RE. 2006. Reward-related decision-making in pediatric major depressive disorder: an fMRI study. J Child Psychol Psychiatry. 47:1031–1040.
Fox MD, Raichle ME. 2007. Spontaneous fluctuations in brain activity observed with functional magnetic resonance imaging. Nat Rev Neurosci. 8:700–711.
Fox MD, Snyder AZ, Vincent JL, Corbetta M, Van E, Raichle ME. 2005. The human brain is intrinsically organized into dynamic, anticorrelated functional networks. Proc Natl Acad Sci USA. 102: 9673–9678.
Fransson P. 2005. Spontaneous low-frequency BOLD signal fluctuations: an fMRI investigation of the resting-state default mode of brain function hypothesis. Hum Brain Mapp. 26:15–29.
Garavan H, Hester R, Murphy K, Fassbender C, Kelly C. 2006. Individual differences in the functional neuroanatomy of inhibitory control. Brain Res. 1105:130–142.
Gavrilescu M, Shaw ME, Stuart GW, Eckersley P, Svalbe ID, Egan GF. 2002. Simulation of the effects of global normalization procedures in functional MRI. Neuroimage. 17:532–542.
Gerardin E, Pochon JB, Poline JB, Tremblay L, Van de Moortele PF, Levy R, Dubois B, Le BD, Lehericy S. 2004. Distinct striatal regions support movement selection, preparation and execution. Neuroreport. 15:2327–2331.
Greicius MD, Krasnow B, Reiss AL, Menon V. 2003. Functional connectivity in the resting brain: a network analysis of the default mode hypothesis. Proc Natl Acad Sci USA. 100:253–258.
Haber SN. 2003. The primate basal ganglia: parallel and integrative networks. J Chem Neuroanat. 26:317–330.
Haber SN, Fudge JL, McFarland NR. 2000. Striatonigrostriatal pathways in primates form an ascending spiral from the shell to the dorsolateral striatum. J Neurosci. 20:2369–2382.
Haber SN, Kim KS, Mailly P, Calzavara R. 2006. Reward-related cortical inputs define a large striatal region in primates that interface with associative cortical connections, providing a substrate for incentive-based learning. J Neurosci. 26: 8368–8376.
Haber SN, Kunishio K, Mizobuchi M, Lynd-Balta E. 1995. The orbital and medial prefrontal circuit through the primate basal ganglia. J Neurosci. 15:4851–4867.
Heimer L, Alheid GF. 1991. Piecing together the puzzle of basal forebrain anatomy. Adv Exp Med Biol. 295:1–42.
Ilinsky IA, Jouandet ML, Goldman-Rakic PS. 1985. Organization of the nigrothalamocortical system in the rhesus monkey. J Comp Neurol. 236:315–330.

Kelly CAM, Uddin LQ, Biswal BB, Castellanos FX, Milham MP. 2008. Competition between functional brain networks mediates behavioral variability. Neuroimage. 39:527–537.
Kelly RM, Strick PL. 2004. Macro-architecture of basal ganglia loops with the cerebral cortex: use of rabies virus to reveal multisynaptic circuits. Prog Brain Res. 143:449–459.
Kemp JM, Powell TP. 1971. The connexions of the striatum and globus pallidus: synthesis and speculation. Philos Trans R Soc Lond B Biol Sci. 262:441–457.
Kiehl KA, Liddle PF, Hopfinger JB. 2000. Error processing and the rostral anterior cingulate: an event-related fMRI study. Psychophysiology. 37:216–223.
Knutson B, Cooper JC. 2005. Functional magnetic resonance imaging of reward prediction. Curr Opin Neurol. 18:411–417.
Kunishio K, Haber SN. 1994. Primate cingulostriatal projection: limbic striatal versus sensorimotor striatal input. J Comp Neurol. 350:337–356.
Kunzle H. 1975. Bilateral projections from precentral motor cortex to the putamen and other parts of the basal ganglia. An autoradiographic study in Macaca fascicularis. Brain Res. 88: 195–209.
Kunzle H. 1977. Projections from the primary somatosensory cortex to basal ganglia and thalamus in the monkey. Exp Brain Res. 30:481–492.
Kunzle H, Akert K. 1977. Efferent connections of cortical, area 8 (frontal eye field) in Macaca fascicularis. A reinvestigation using the autoradiographic technique. J Comp Neurol. 173:147–164.
Lafer B, Renshaw PF, Sachs GS. 1997. Major depression and the basal ganglia. Psychiatr Clin North Am. 20:885–896.
Leh SE, Ptito A, Chakravarty MM, Strafella AP. 2007. Fronto-striatal connections in the human brain: a probabilistic diffusion tractography study. Neurosci Lett. 419:113–118.
Lehericy S, Ducros M, Van de Moortele PF, Francois C, Thivard L, Poupon C, Swindale N, Ugurbil K, Kim DS. 2004. Diffusion tensor fiber tracking shows distinct corticostriatal circuits in humans. Ann Neurol. 55:522–529.
Lepsien J, Nobre AC. 2006. Cognitive control of attention in the human brain: insights from orienting attention to mental representations. Brain Res. 1105:20–31.
MacDonald AW, 3rd, Cohen JD, Stenger VA, Carter CS. 2000. Dissociating the role of the dorsolateral prefrontal and anterior cingulate cortex in cognitive control. Science. 288:1835–1838.
Macey PM, Macey KE, Kumar R, Harper RM. 2004. A method for removal of global effects from fMRI time series. Neuroimage. 22:360–366.
Margulies DS, Kelly AM, Uddin LQ, Biswal BB, Castellanos FX, Milham MP. 2007. Mapping the functional connectivity of anterior cingulate cortex. Neuroimage. 37:579–588.
Mayberg HS, Lozano AM, Voon V, McNeely HE, Seminowicz D, Hamani C, Schwalb JM, Kennedy SH. 2005. Deep brain stimulation for treatment-resistant depression. Neuron. 45:651–660.
McClure SM, Berns GS, Montague PR. 2003. Temporal prediction errors in a passive learning task activate human striatum. Neuron. 38:339–346.
Middleton FA, Strick PL. 1994. Anatomical evidence for cerebellar and basal ganglia involvement in higher cognitive function. Science. 266:458–461.
Middleton FA, Strick PL. 2000a. Basal ganglia and cerebellar loops: motor and cognitive circuits. Brain Res Brain Res Rev. 31: 236–250.
Middleton FA, Strick PL. 2000b. Basal ganglia output and cognition: evidence from anatomical, behavioral, and clinical studies. Brain Cogn. 42:183–200.
Middleton FA, Strick PL. 2002. Basal-ganglia 'projections' to the prefrontal cortex of the primate. Cereb Cortex. 12:926–935.
Milham MP, Banich MT. 2005. Anterior cingulate cortex: an fMRI analysis of conflict specificity and functional differentiation. Hum Brain Mapp. 25:328–335.
Milham MP, Banich MT, Barad V. 2003. Competition for priority in processing increases prefrontal cortex's involvement in top-down control: an event-related fMRI study of the stroop task. Brain Res Cogn Brain Res. 17:212–222.
Monchi O, Petrides M, Strafella AP, Worsley KJ, Doyon J. 2006. Functional role of the basal ganglia in the planning and execution of actions. Ann Neurol. 59:257–264.
Montoya A, Price BH, Menear M, Lepage M. 2006. Brain imaging and cognitive dysfunctions in Huntington's disease. J Psychiatry Neurosci. 31:21–29.
Morcom AM, Fletcher PC. 2006. Does the brain have a baseline? Why we should be resisting a rest. Neuroimage. 37:1073–1082.
Nobre AC, Coull JT, Maquet P, Frith CD, Vandenberghe R, Mesulam MM. 2004. Orienting attention to locations in perceptual versus mental representations. J Cogn Neurosci. 16:363–373.
O'Doherty J, Dayan P, Schultz J, Deichmann R, Friston K, Dolan RJ. 2004. Dissociable roles of ventral and dorsal striatum in instrumental conditioning. Science. 304:452–454.
Parent A, Hazrati LN. 1995. Functional anatomy of the basal ganglia. I. The cortico-basal ganglia-thalamo-cortical loop. Brain Res Brain Res Rev. 20:91–127.
Parent M, Levesque M, Parent A. 1999. The pallidofugal projection system in primates: evidence for neurons branching ipsilaterally and contralaterally to the thalamus and brainstem. J Chem Neuroanat. 16:153–165.
Paus T, Koski L, Caramanos Z, Westbury C. 1998. Regional differences in the effects of task difficulty and motor output on blood flow response in the human anterior cingulate cortex: a review of 107 PET activation studies. Neuroreport. 9:R37–R47.
Postle BR, D'Esposito M. 2003. Spatial working memory activity of the caudate nucleus is sensitive to frame of reference. Cogn Affect Behav Neurosci. 3:133–144.
Postuma RB, Dagher A. 2006. Basal ganglia functional connectivity based on a meta-analysis of 126 positron emission tomography and functional magnetic resonance imaging publications. Cereb Cortex. 16:1508–1521.
Powell EW, Leman RB. 1976. Connections of the nucleus accumbens. Brain Res. 105:389–403.
Reiss JP, Campbell DW, Leslie WD, Paulus MP, Stroman PW, Polimeni JO, Malcolmson KA, Sareen J. 2005. The role of the striatum in implicit learning: a functional magnetic resonance imaging study. Neuroreport. 16:1291–1295.
Rolls ET. 2000. The orbitofrontal cortex and reward. Cereb Cortex. 10:284–294.
Rubia K, Smith AB, Woolley J, Nosarti C, Heyman I, Taylor E, Brammer M. 2006. Progressive increase of frontostriatal brain activation from childhood to adulthood during event-related tasks of cognitive control. Hum Brain Mapp. 27:973–993.
Sagvolden T, Johansen EB, Aase H, Russell VA. 2005. A dynamic developmental theory of attention-deficit/hyperactivity disorder (ADHD) predominantly hyperactive/impulsive and combined subtypes. Behav Brain Sci. 28:397–419.
Scheres A, Milham MP, Knutson B, Castellanos FX. 2007. Ventral striatal hyporesponsiveness during reward anticipation in attention-deficit/hyperactivity disorder. Biol Psychiatry. 61:720–724.
Schultz W, Tremblay L, Hollerman JR. 2000. Reward processing in primate orbitofrontal cortex and basal ganglia. Cereb Cortex. 10:272–284.
Selemon LD, Goldman-Rakic PS. 1985. Longitudinal topography and interdigitation of corticostriatal projections in the rhesus monkey. J Neurosci. 5:776–794.
Shenton ME, Dickey CC, Frumin M, McCarley RW. 2001. A review of MRI findings in schizophrenia. Schizophr Res. 49:1–52.
Sonuga-Barke EJ. 2005. Causal models of attention-deficit/hyperactivity disorder: from common simple deficits to multiple developmental pathways. Biol Psychiatry. 57:1231–1238.
Sridharan D, Levitin DJ, Chafe CH, Berger J, Menon V. 2007. Neural dynamics of event segmentation in music: converging evidence for dissociable ventral and dorsal networks. Neuron. 55:521–532.
Stein DJ, Goodman WK, Rauch SL. 2000. The cognitive-affective neuroscience of obsessive-compulsive disorder. Curr Psychiatry Rep. 2:341–346.
Talairach J, Tournoux P. 1988. Co-planar stereotaxic atlas of the human brain: 3-dimensional proportional system: an approach to cerebral imaging. Stuttgart: G. Thieme.

Uddin LQ, Kelly AMC, Biswal BB, Castellanos FX, Milham MP. Forthcoming. Functional connectivity of default mode network components: correlation, anticorrelation, and causality. Hum Brain Mapp.
Ullsperger M, von Cramon DY. 2004. Neuroimaging of performance monitoring: error detection and beyond. Cortex. 40:593–604.
van Veen V, Cohen JD, Botvinick MM, Stenger VA, Carter CS. 2001. Anterior cingulate cortex, conflict monitoring, and levels of processing. Neuroimage. 14:1302–1308.
Volkow ND, Wang GJ, Begleiter H, Porjesz B, Fowler JS, Telang F, et al. 2006. High levels of dopamine D2 receptors in unaffected members of alcoholic families: possible protective factors. Arch Gen Psychiatry. 63:999–1008.
Weissman DH, Warner LM, Woldorff MG. 2004. The neural mechanisms for minimizing cross-modal distraction. J Neurosci. 24:10941–10949.
Wessa M, Houenou J, Paillere-Martinot ML, Berthoz S, Artiges E, Leboyer M, Martinot JL. 2007. Fronto-striatal overactivation in euthymic bipolar patients during an emotional go/nogo task. Am J Psychiatry. 164:638–646.
Wichmann T, DeLong MR. 2006. Basal ganglia discharge abnormalities in Parkinson's disease. J Neural Transm Suppl. 70:21–25.
Yeterian EH, Van Hoesen GW. 1978. Cortico-striate projections in the rhesus monkey: the organization of certain cortico-caudate connections. Brain Res. 139:43–63.